Published in final edited form as:
Nat Biotechnol. 2005 June ; 23(6): 725–730.

Intermolecular complementation achieves high specificity tumor targeting by anthrax toxin

Shihui Liu[1], **Vivien Redeye**[2], **Jeffrey G. Kuremsky**[1], **Marissa Kuhnen**[2], **Alfredo Molinolo**[2], **Thomas H. Bugge**[2,*], and **Stephen H. Leppla**[1,*]

1*Microbial Pathogenesis Section, National Institute of Allergy and Infectious Diseases, National Institutes of Health, Bethesda, MD 20892*

2*Oral and Pharyngeal Cancer Branch, National Institute of Dental and Craniofacial Research, National Institutes of Health, Bethesda, MD 20892*

Abstract

Anthrax toxin protective antigen (PrAg) forms a heptamer in which the binding site for lethal factor (LF) spans two adjacent monomers[1,2]. This suggested that high cell-type specificity in tumor targeting could be obtained using monomers that generate functional LF binding sites only through intermolecular complementation. PrAg mutants were produced having mutations in different LF binding subsites and containing either urokinase plasminogen activator (uPA) or matrix metalloproteinases (MMP) cleavage sites. Individually, these PrAg mutants had low toxicity due to impaired LF binding, but when administered together to uPA- and MMP-expressing tumor cells, they assembled into functional LF-binding heteroheptamers. The mixture of two complementing PrAg variants had greatly reduced toxicity to mice and was highly effective in treatment of aggressive transplanted tumors of diverse origin. These results show that anthrax toxin, and by implication, other multimeric toxins, offer unique opportunities to introduce multiple specificity determinants, thereby achieving high therapeutic indices.

Keywords

Anthrax toxin; cytotoxins; furin; LF; matrix metalloproteinases; protective antigen; tumor targeting; urokinase plasminogen activator

Anthrax toxin, the major virulence factor of *Bacillus anthracis*, consists of three polypeptides: protective antigen (PrAg), lethal factor (LF), and edema factor (EF)[3]. These three individually non-toxic proteins can assemble at the mammalian cell surface into toxic complexes. To intoxicate host cells, PrAg binds to its cellular receptors[4,5], and is subsequently cleaved by furin or furin-like proteases after the sequence RKKR[167], allowing the receptor-bound carboxyl-terminal 63-kDa fragment (PrAg63) to form a ring-shaped heptamer[6,7]. The oligomerization of PrAg63 provides the binding site for LF and EF[1,2], and triggers internalization of the toxin complex into endosomes where LF and EF translocate to the cytosol to exert their cytotoxic effects[8,9]. The unique requirement that PrAg be activated on the target cell surface provides a way to re-engineer this protein to make its activation dependent on proteases that are enriched on the surface of the tumor cells. We previously generated PrAg proteins requiring activation by either MMP[10] or uPA[11,12]. Both these protease systems are overproduced by tumor tissues and are implicated in cancer cell growth and metastasis[13-15]. The MMP- or uPA-activated PrAg proteins were greatly attenuated in their toxicity to normal tissues and showed potent tumoricidal activities in mice when co-administrated with fusion

*Correspondence should be addressed to: Thomas H. Bugge (thomas.bugge@nih.gov) or Stephen H. Leppla (sleppla@niaid.nih.gov)

protein FP59, which consists of anthrax LF amino acids 1-254 fused to the ADP-ribosylation domain of *Pseudomonas* exotoxin A[16].

Recent studies showed that LF and EF bind only to the oligomeric form of PrAg63[1]. It follows that the binding site must span two adjacent monomers. Mutagenesis studies assigned certain PrAg residues involved in LF binding to either of three subsites: subsite I (Arg^{178}) and subsite III (Ile^{207}, Ile^{210}, and Lys^{214}) in the clockwise (righthand) subunit, and subsite II (Lys^{197} and Arg^{200}) in the counterclockwise (lefthand) subunit[1,2] (Fig. 1). In this report, we have exploited these findings to design PrAg proteins to achieve high cell-type specificity. The strategy used is diagrammed in Figure 1. The top row shows the assembly of native PrAg63 into a heptamer having functional LF binding sites. The second row shows a PrAg mutant altered in the protease cleavage site so as to be dependent on MMP activity, and containing a second mutation that inactivates LF binding subsite III. Binding of this PrAg to an MMP-expressing cells leads to assembly of a heptamer in which every LF binding site contains the inactivating subsite III mutation. The third row shows a PrAg protein requiring uPA activation and having an inactivating LF binding subsite II mutation. It would also produce an impaired heptamer. However, adding a mixture of these PrAg proteins to a cell having both MMP and uPA activities would generate two PrAg63 proteins that can randomly assemble into a heptamer in which up to three of the LF binding sites would bind LF (the fourth row).

To determine whether intermolecular complementation can restore an active LF binding site, we constructed mutated PrAg proteins PrAg-R200A and PrAg-I210A that contain alanine substitutions at, respectively, the LF-binding subsite II residue Arg^{200} and the subsite III residue Ile^{210}. These mutated proteins are designated as belonging to groups L and R, respectively, indicating the location of the mutations relative to the monomer-monomer interface. PrAg-200A and PrAg-I210A, just like wild-type PrAg, bound to Chinese hamster ovary (CHO) cells, were processed by furin to produce PrAg63, and formed SDS-resistant heptamers (Fig. 2a, top panel), but they had significantly decreased LF binding (Fig. 2a, lower panel). However, when PrAg-200A and PrAg-I210A were applied together to CHO cells, LF-binding ability was substantially regained (Fig. 2a). Therefore, PrAg-R200A and PrAg-I210A display intermolecular complementation in formation of LF-binding PrAg heptamers. The decreased LF binding observed for the PrAg-R200A/PrAg-I210A mixture is expected (Fig. 2a), because the PrAg63 heptamer formed from wild-type PrAg is able to bind three LF molecules[1,17], while heptamers formed from the complementing PrAg proteins will on average contain fewer than three functional sites (Fig. 1). In agreement with the results of Figure 2a, cytotoxicity measurements showed that PrAg-R200A and PrAg-I210A demonstrated intermolecular complementation in killing of the murine macrophage cell line RAW264.7 by LF (Fig. 2c). The mixture of PrAgR200A/PrAg-I210A had an EC_{50} for LF of 0.2 nM (18 ng/ml), 14- and 10-fold lower than that of PrAg-R200A (2.7 nM) and PrAg-I210A (2.0 nM) (Fig. 2d,e), respectively, and approaching the potency found with wild-type PrAg, 0.05 nM (Fig. 2b).

The apparent affinities of the LF binding sites present on the PrAg heptamers formed by these mutated PrAg proteins were measured by competitive Schild plot analyses[18,19]. Cytotoxicity assays were performed using as a competitor a mutated, non-toxic LF protein, LFE687C [20], that contains a cysteine substitution at the catalytic site Glu^{687} (Fig. 2b-f). Addition of fixed concentrations of LF-E687C shifted the cytotoxicity dose-response curves rightward (Fig. 2b-e). A reciprocal plot of the midpoints of the dose response curves yields apparent dissociation constants for the affinity of LF-E687C to the PrAg heptamers (Fig. 2f). The apparent K_d for LF-E687C binding to the complementing mixture of PrAg-R200A and PrAg-I210A is 0.26 nM, 39- and 18-fold lower than those of the individual proteins (10.3 nM for PrAg-R200A, 4.7 nM for PrAg-I210A), and approaching that of wild-type PrAg, 0.15 nM (Fig. 2f).

The evidence that intermolecular complementation does occur in this system implied that a PrAg mixture could be created that would be toxic only to cells expressing two distinct cell-surface proteolytic activities. To test this hypothesis, the previously characterized uPA-activated PrAg-U2 (with the furin site RKKR changed to uPA cleavage sequence PGSGRSA) [11,12], was further mutated to yield the group L proteins PrAg-U2-K197A and PrAg-U2-R200A (Fig. 1, Supplementary Table 1 online). Similarly, the previously described PrAg-L1 protein (with the furin site changed to MMP cleavage sequence GPLGMLSQ)[10] was further mutated to yield the group R proteins PrAg-L1-R178A, PrAg-L1-I210A, and PrAg-L1-K214A. PrAg proteins from the L and R groups were added individually and in combination to human melanoma A2058 cells along with the effector FP59. The results showed that the group L protein PrAg-U2-R200A complemented the group R proteins, in particular PrAg-L1-I210A, to efficiently kill A2058 cells in a wide range of molar ratios from 1:5 to 5:1 (Fig. 3a). In contrast, PrAg-U2-R200A, PrAg-L1-I210A, PrAg-L1-K214A, and PrAg-L1-R178A killed ≤ 50% of the tumor cells when used alone at high concentrations (7.2 nM), demonstrating that their cytotoxic action is greatly increased by intermolecular complementation. Surprisingly, PrAg-U2-K197A could not complement the proteins in the group R (data not shown). In fact, Lys ^{197} is very close to the LF-binding subsite III residue Lys^{214} in the PrAg crystal structure. Thus, Lys ^{197} may also be a part of subsite III, so that the Lys^{197} residues in two adjacent PA63 subunits would be required for LF binding. This would also provide another explanation for the fact that the PrAg heptamer can bind a maximum of only three LF or EF molecules[1,17].

To verify that the cytotoxicity of PrAg-U2-R200A/PrAg-L1-I210A mixture is dependent on both uPA and MMP activities, we first showed that, in contrast to wild-type PrAg, PrAg-U2-R200A and PrAg-L1-I210A could not be cleaved by furin (Fig. 3b), but instead, were cleaved only by uPA and MT1 (membrane-type 1)-MMP, respectively, to produce PrAg63 (Fig. 3b). We then further demonstrated that the cytotoxicity of the combination of PrAg-U2-R200A and PrAg-L1-I210A was greatly inhibited by plasminogen activator inhibitor 1 (PAI-1), and tissue inhibitor 2 of MMP (TIMP-2) (Fig. 3c), with either one being sufficient, demonstrating that the toxicity was dependent on the simultaneous expression by the tumor cells of both uPA and MMP activities.

To evaluate the *in vivo* toxicity of the PrAg proteins described here, various doses of mutated PrAg proteins were injected intraperitoneally into C57BL6 mice at days 0, 3, and 6 in the presence of 3 μg FP59. Wild-type PrAg was very toxic, having a maximum tolerated dose/three injections (MTD3) of 0.25 μg. PrAg-L1 was about 16-fold attenuated (MTD3 = 4 μg), and PrAg-U2 40-fold attenuated (MTD3 = 10 μg). The toxicities of PrAg-L1-I210A (MTD3 = 50 μg) and PrAg-U2-R200A (MTD3 ≥ 100 μg) were further decreased about 10-fold when compared with that of PrAg-L1 and PrAg-U2, respectively (Supplementary Table 1 online). Interestingly, PrAg-U2-R200A and PrAg-L1-I210A demonstrated an intermolecular complementation in toxicity to mice (MTD3 = 30 + 15 μg) (Supplementary Table 1 online), but the toxicity was substantially decreased compared with PrAg-U2 (MTD3 = 10 μg) and PrAg-L1 (MTD3 = 4 μg). To identify the tissues targeted by this mixture, mice were treated intraperitoneally with a combination of 45 μg PrAg-U2-R200A and 22.5 μg PrAg-L1-I210A in the presence of 3 μg FP59 at day 0, 3, and 6 (1.5×MTD3). Full necropsy analyses of these mice did not uncover any gross abnormalities. However, extensive histological analyses revealed areas of necrosis in bone and bone marrow (Supplementary Fig. 1 online), with no other damage found in all other organs and tissues examined (listed in **METHODS**). Mice treated with 1×MTD3 showed no outward signs of illness or gross abnormalities, and the localized necrosis in bone and bone marrow was reduced in severity (data not shown).

We next evaluated the PrAg-U2-R200A and PrAg-L1-I210A combination in treatment of three mouse tumors, B16-BL6 melanoma, T241 fibrosarcoma, and LL3 Lewis lung carcinoma. Mice bearing intradermal tumor nodules (0.1-0.8% of body mass) were treated with PBS, 6 μg PrAg-

U2-R200A, 6 μg PrAg-L1-I210A, or with a combination of 3 μg PrAg-U2-R200A and 3 μg PrAg-L1-I210A in the presence of 0.5 μg FP59 at day 0, 3, and 6, by injection adjacent to the tumor nodules. The combination of PrAg-U2-R200A/PrAg-L1-I210A had strong anti-tumor activity, causing reductions in tumor size of 94 % ($p < 0.001$) in B16-BL6 melanoma, 92% ($p < 0.001$) for T241 fibrosarcoma, and 71% ($p < 0.001$) for Lewis lung carcinoma, as compared to PBS-treated tumors at the time of euthanization (day 8 for melanoma and carcinoma, day 10 for fibrosarcoma) (Fig. 4a-e). In contrast, the tumors showed little or no response to treatment with the individual proteins. These data demonstrate that the potent tumoricidal activity of these engineered PrAg proteins requires their intermolecular complementation.

To directly compare the anti-tumor efficacy of this intermolecular complementation with that of PrAg-U2, B16-BL6 tumor-bearing mice were treated intradermally with 2 μg or 6 μg of PrAg-U2 or the mixture of PrAg-U2-R200A and PrAg-L1-I210A (1 μg + 1 μg and 3 μg + 3 μg, respectively) in the presence of 0.5 μg FP59 at day 0, 3, and 6. The experiment showed that the combination of PrAg-U2-R200A and PrAg-L1-I210A was at least as effective as PrAg-U2 (Fig. 4f). Given that the MTD3 of PrAg-U2-R200A/PrAg-L1-I210A is 4.5-fold higher than that of PrAg-U2, these data show that the complementing mixture of PrAg-U2-R200A and PrAg-L1-I210A achieves higher tumor specificity. B16-BL6 melanoma-bearing mice were also treated intraperitoneally with the mixture of 20 μg PrAg-U2-R200A and 10 μg PrAg-L1-I210A in the presence of 3 μg FP59 at day 0, 3, and 6 (2/3 MTD3). This systemic treatment significantly reduced tumor growth (60 % reduction in size) ($p < 0.01$), achieving results equivalent to that obtained by local administration of 2 μg of the mixture of PrAg-U2-R200A and PrAg-L1-I210A (Fig. 4f). A moderate body weight loss was observed only in the systemic treatment group (23.9±1.5 g prior treatment to 21.8±1.4 g post treatment, $p < 0.05$) (Fig. 4g).

This work establishes proof of principle that anthrax toxin can be reengineered so that its cytotoxicity relies on two distinct proteolytic activities that are overproduced by tumor tissues, thus achieving enhanced specificity for tumors. The human genome encodes approximately 550 functional proteolytic enzymes; two thirds of which would be predicted to function in the pericellular environment[21]. Recent high throughput expression profiling has shown that human tumors present unique molecular “signatures” in the form of distinct combinations of genes that are consistently overexpressed within a particular tumor type. This also includes pericellular proteases that are expressed by tumor cells in combinations not found in normal tissues[22-26]. The methodology presented here therefore enables the development of engineered toxins with exquisite specificity for certain human tumor types. For example, toxins activated by combinations of hepsin with either matriptase or prostate specific antigen (PSA) [27] would be predicted to be exceedingly selective for prostate carcinoma.

METHODS

Construction of mutated PrAg proteins

A modified overlap PCR method was used to construct the two groups of mutated PrAg proteins. The group L included two uPA-activated PrAg proteins, PrAg-U2-K197A and PrAg-U2-R200A, in which LF-binding subsite II residues Lys^{197} and Arg^{200} were changed to Ala. The group R contained three MMP-activated PrAg proteins, PrAg-L1-R178A, PrAg-L1-I210A, and PrAg-L1-K214A, in which the LF-binding subsite I (Arg^{178}) or subsite III (Ile^{210} and Lys^{214}) were changed to Ala. To amplify DNA for the group L mutants, PrAg-U2 expression plasmid pYS5-PrAg-U2[11] was used as a template. We used a sense primer Pn (GGTAGATGACCAAGAAGTGA) and an antisense primer Pk197a (AAAT*CCATGG*TGAAAGAAAAGTTCTTTTATTTGCGACATCAACCGTATATCC, *Nco*I site is in italic, the antisense codon for Ala^{197} instead of Lys^{197} underlined) to amplify a mutagenic fragment K197A. We used the primer Pn and an antisense primer Pr200a (AAAT*CCATGG*TGAAAGAAAAGTTGCTTTATTTTTGACATCAACCG, the antisense

codon for Ala^{200} instead of Arg^{200} underlined) to amplify a mutagenic fragment R200A. We used a sense primer Pnco (TTCA*CCATGG*ATTTCTAATATTCATG, *Nco*I site is in italic) and an antisense primer Ppst (TAAATC*CTGCAG*ATACACTCCCACCAAT, *Pst*I site is in italic) to amplify a fragment designated NP. After digestion by *Nco*I, the fragments K197A and NP, and R200A and NP were ligated. The primers Pn and Ppst were used to amplify the ligated products of K197A + NP and R200A + NP, respectively, resulting in the mutagenized fragments U2-K197A and U2-R200A.

To amplify the group R mutants, PrAg-L1 expression plasmid pYS5-PrAg-L1[10] was used as a template. We used primer Pn and an antisense primer Pr178a-1 (AG*GGATCC*CATCATTGTCAGCGTCTGGAACCGTAGGTCC, *Bam*HI site is in italic, the antisense codon for Ala^{178} instead of Arg^{178} underlined) to amplify a mutagenic fragment R178A-1. We used a sense primer Pr178a-2 (TG*GGATCC*CTGATTCATTAGAGGTAGAAGG, *Bam*HI site is in italic, the codon for Ala^{178} instead of Arg^{178} underlined) and the primer Ppst to amplify a fragment R178A-2. After digestion by *BamH*I, the fragments R178A-1 and R178A-2 were ligated. The primers Pn and Ppst were used to amplify their ligated product, resulting in the mutagenized fragments L1-R178A.

We used the primer Pn and Ppst to amplify a fragment designated PP. We used a sense primer Pi210a (TTCA*CCATGG*ATTTCTAATGCTCATGAAAAGAAAGG, *Nco*I site is in italic, the codon for Ala^{210} instead of Ile^{210} underlined) and an antisense primer Pli4 (ACGTTTATCTCTTATTAAAAT) to amplify a mutagenic fragment I210A. We used a sense primer Pk214a (TTCA*CCATGG*ATTTCTAATATTCATGAAAAGGCAGGATTAACCAAATATA, *Nco*I site is in italic, the codon for Ala^{214} instead of Lys^{214} underlined) and the primer Pli4 to amplify a mutagenic fragment K214A. After digestion by *Nco*I, the fragments I210A and PP, and I214A and PP were ligated. Primers Pn and Pli4 were used to amplify the ligated products of I210A + PP and I214A + PP, respectively, resulting in the mutagenized fragments L1-I210A and L1-K214A.

The 670-bp *Hin*dIII/*Pst*I fragments from the digests of U2-K197A, U2-R200A, L1-R178A, L1-I210A, and L1-K214A were cloned between the *Hin*dIII and *Pst*I sites of pYS5, a wild-type PrAg expression plasmid. The resulting mutated PrAg proteins were accordingly named PrAg-U2-K197A, PrAg-U2-R200A, PrAg-L1-R178A, PrAg-L1-I210A, and PrAg-L1-K214A. We also constructed PrAg-R200A and PrAg-I210A, using procedures similar to those described above except that plasmid pYS5 was used as a template for PCR. The sequences of all mutated PrAg constructs were confirmed by DNA sequencing.

Expression and purification of PrAg proteins

Plasmids encoding the constructs described above were transformed into the non-virulent strain *Bacillus anthracis* BH445, and transformants were grown in FA medium[28] with 20 μg/ml kanamycin and 10 μg/ml chloramphenicol for 12 h at 37°C. The proteins were secreted into the culture supernatants at 20-40 mg/L, precipitated by ammonium sulfate, and purified by gel filtration chromatography to one prominent band at the expected molecular mass of 83 kDa, which co-migrated with wild-type PrAg in SDS-PAGE.

Cytotoxicity assays with MTT

Human melanoma A2058 cells were grown and maintained as described previously[10,29]. In tumor tissues, cancer cells typically overexpress uPAR, while either the cancer cells or the adjacent tumor stromal cells express pro-uPA, which is activated on the cancer cell surface after binding to uPAR[14]. A2058 cells express both uPAR and MMP but do not express pro-

uPA under the current culture condition[10,11]. Therefore, pro-uPA was added to mimic the *in vivo* situation. Cells were cultured in 96-well plates to approximately 50% confluence. Then the cells were pre-incubated for 30 min with 1.9 nM pro-uPA (#107, American Diagnostica Inc., Greenwich, CT) with or without PAI-1 (46 nM) (#1094, American Diagnostica Inc.) or TIMP-2 (0.4 μM) (Cat. No. PF021, Calbiochem, San Diego, CA). Various concentrations of PrAg proteins or mixtures of them, combined with FP59 (1.9 nM), were added to the cells to give a total volume of 200 μl/well. Cell viability was assayed after incubation for 48 h using MTT (3-[4,5-dimethylthiazol-2-yl]-2,5-diphenyltetrazolium bromide) as described previously[10].

Murine macrophage RAW264.7 cells were grown in Dulbecco's Modified Essential Medium (DMEM) with 0.45% glucose, 10% fetal bovine serum (FCS), 2 mM glutamine, and 50 μg/ml gentamicin. RAW264.7 cells cultured in 96-well plates to approximately 80% confluence were incubated with 6 nM of different PrAg proteins or their combinations and various amounts of LF (0-12 nM) for 3.5 h, and then MTT was added to determine cell viability.

PrAg-mediated LF-binding assay

CHO cells grown in 24-well plates were incubated with 12 nM of different PrAg proteins or their combinations and 1.2 nM of LF for 2 h at 37°C. Then the cells were washed and lysed in a modified RIPA lysis buffer containing protease inhibitors[29]. The cell lysates were analyzed by SDS-PAGE followed by Western blotting using a rabbit anti-PrAg antiserum (serum #5308, made in our laboratory) to detect PrAg binding and processing, or a rabbit anti-LF antiserum (serum #5309, made in our laboratory) to detect LF binding.

In vitro cleavage of PrAg proteins by furin, uPA and MT1-MMP

Reaction mixtures of 50 μl containing 3 μg of the PrAg proteins were incubated at 37°C with 1 unit of furin (Product No. F2677, Sigma, Saint Louis, MO), 0.3 μg uPA (#124, American Diagnostica Inc., Greenwich, CT), or 0.3 μg soluble MT1-MMP (Calbiochem). Digestion with furin and uPA was performed as described[11]. Cleavage with MT1-MMP was done in 50 mM HEPES, pH 7.5, 10 mM $CaCl_2$, 200 mM NaCl, 0.05% Brij35, 50 μM $ZnSO_4$. Aliquots withdrawn at intervals were analyzed by SDS-PAGE, and proteins were visualized by Western blot analysis using the rabbit anti-PrAg polyclonal antiserum (serum #5308).

Determination of the maximum tolerated doses of recombinant toxins

Male and female C57BL/6J mice (The Jackson Laboratory) aged between 6-8 weeks were housed in a pathogen-free facility certified by the Association for Assessment and Accreditation of Laboratory Animal Care International, and the study was carried out in accordance with institutional guidelines. The maximum tolerated doses of PrAg proteins were determined using a dose escalation protocol aimed at minimizing the number of the mice to be used. The mice (n = 5) in each group were anesthetized by Isoflurane inhalation and injected intraperitoneally with three doses of various PrAg proteins combined with 3 μg FP59 in 500 μl PBS at days 0, 3, and 6. The mice were monitored closely for signs of toxicity including inactivity, loss of appetite, inability to groom, ruffling of fur, and shortness of breath, and euthanized by CO_2 inhalation at the onset of obvious malaise. The maximum tolerated doses for three administrations (MTD3) were determined as the highest doses in which outward disease was not observed in any mice within a 14-day period of observation. The significance of differences between treatment groups was determined by two-tailed Chi-square analysis.

Histopathological analysis

Mice were injected with PBS (n = 3) or the mixture of PrAg-U2-R200A/PrAg-L1-I210A (45/22.5 μg (n = 5) or 30/15 μg (n = 3), in the presence of 3 μg FP59) in PBS at day 0, 3, and

6. At day 7, the mice were killed by a brief CO_2 inhalation. The organs and tissues, including brain, lung, heart, liver, small and large intestines, kidney and adrenal, stomach, pancreases, spleen, thyroid, bladder, esophagus, skeletal muscles, thymus, lymph nodes, etc., were fixed for 24 h in 4% paraformaldehyde, embedded in paraffin, sectioned, and stained with hematoxylin/eosin and subjected to microscopic analysis by a pathologist unaware of the treatments.

Tumor transplantation and toxin treatment experiments

The transplanted murine B16-BL6 melanoma, T241 fibrosarcoma and LL3 Lewis lung carcinoma were established subcutaneously as described previously [12]. PrAg proteins combined with 0.5 μg FP59 in 100 μl PBS or PBS 100 μl alone were injected intradermally adjacent to the tumor nodule when the tumors had reached a size ranging from approximately 0.1 - 0.8 % of total body mass (day 0) and again at days 3 and 6. In a systemic treatment study, B16-BL6 melanoma-bearing mice were treated intraperitoneally with PBS or the mixture of 20 μg PrAgU2-R200A and 10 μg PrAg-L1-I210A in the presence of 3 μg FP59 at day 0, 3, and 6 (2/3 MTD3). The longest and shortest tumor diameter was determined daily by calipation by an investigator unaware of treatment group, and the tumor weight was calculated using the formula milligrams = (length in mm ×[width in mm]^2)/2[30]. The experiment was terminated when one or more mice in a treatment group presented frank tumor ulceration or exceed 10% of body weight. The significance of differences in tumor size was determined by two-tailed Student's t-test.

Supplementary Material

Refer to Web version on PubMed Central for supplementary material.

ACKNOWLEDGMENTS

We thank Dana Hsu for assistance with toxin purification.

References

1. Mogridge J, Cunningham K, Lacy DB, Mourez M, Collier RJ. The lethal and edema factors of anthrax toxin bind only to oligomeric forms of the protective antigen. Proc. Natl. Acad. Sci. U. S. A 2002;99:7045–7048. [PubMed: 11997437]
2. Cunningham K, Lacy DB, Mogridge J, Collier RJ. Mapping the lethal factor and edema factor binding sites on oligomeric anthrax protective antigen. Proc. Natl. Acad. Sci. U. S. A 2002;99:7049–7053. [PubMed: 11997439]
3. Liu S, Schubert RL, Bugge TH, Leppla SH. Anthrax toxin: structures, functions and tumour targeting. Expert. Opin. Biol. Ther 2003;3:843–853. [PubMed: 12880383]
4. Bradley KA, Mogridge J, Mourez M, Collier RJ, Young JA. Identification of the cellular receptor for anthrax toxin. Nature 2001;414:225–229. [PubMed: 11700562]
5. Scobie HM, Rainey GJ, Bradley KA, Young JA. Human capillary morphogenesis protein 2 functions as an anthrax toxin receptor. Proc. Natl. Acad. Sci. U. S. A 2003;100:5170–5174. [PubMed: 12700348]
6. Klimpel KR, Molloy SS, Thomas G, Leppla SH. Anthrax toxin protective antigen is activated by a cell-surface protease with the sequence specificity and catalytic properties of furin. Proc. Natl. Acad. Sci. U. S. A 1992;89:10277–10281. [PubMed: 1438214]
7. Petosa C, Collier RJ, Klimpel KR, Leppla SH, Liddington RC. Crystal structure of the anthrax toxin protective antigen. Nature 1997;385:833–838. [PubMed: 9039918]
8. Leppla SH. Anthrax toxin edema factor: a bacterial adenylate cyclase that increases cyclic AMP concentrations of eukaryotic cells. Proc. Natl. Acad. Sci. U. S. A 1982;79:3162–3166. [PubMed: 6285339]

9. Duesbery NS, Webb CP, Leppla SH, Gordon VM, Klimpel KR, Copeland TD, Ahn NG, Oskarsson MK, Fukasawa K, Paull KD, Vande Woude GF. Proteolytic inactivation of MAP-kinase-kinase by anthrax lethal factor. Science 1998;280:734–737. [PubMed: 9563949]
10. Liu S, Netzel-Arnett S, Birkedal-Hansen H, Leppla SH. Tumor cell-selective cytotoxicity of matrix metalloproteinase-activated anthrax toxin. Cancer Res 2000;60:6061–6067. [PubMed: 11085528]
11. Liu S, Bugge TH, Leppla SH. Targeting of tumor cells by cell surface urokinase plasminogen activator-dependent anthrax toxin. J. Biol. Chem 2001;276:17976–17984. [PubMed: 11278833]
12. Liu S, Aaronson H, Mitola DJ, Leppla SH, Bugge TH. Potent antitumor activity of a urokinase-activated engineered anthrax toxin. Proc. Natl. Acad. Sci. U. S. A 2003;100:657–662. [PubMed: 12525700]
13. Stetler-Stevenson WG, Aznavoorian S, Liotta LA. Tumor cell interactions with the extracellular matrix during invasion and metastasis. Annu. Rev. Cell Biol 1993;9:541–573. [PubMed: 8280471]
14. Dano K, Romer J, Nielsen BS, Bjorn S, Pyke C, Rygaard J, Lund LR. Cancer invasion and tissue remodeling--cooperation of protease systems and cell types. APMIS 1999;107:120–127. [PubMed: 10190288]
15. Andreasen PA, Egelund R, Petersen HH. The plasminogen activation system in tumor growth, invasion, and metastasis. Cell Mol. Life Sci 2000;57:25–40. [PubMed: 10949579]
16. Arora N, Leppla SH. Residues 1-254 of anthrax toxin lethal factor are sufficient to cause cellular uptake of fused polypeptides. J. Biol. Chem 1993;268:3334–3341. [PubMed: 8429009]
17. Mogridge J, Cunningham K, Collier RJ. Stoichiometry of anthrax toxin complexes. Biochemistry 2002;41:1079–1082. [PubMed: 11790132]
18. Malatynska E, Crites G, Yochum A, Kopp R, Giroux ML, Dilsaver SC. Schild regression analysis of antidepressant and bicuculline antagonist effects at the GABAA receptor. Pharmacology 1998;57:117–123. [PubMed: 9691231]
19. Varughese M, Teixeira AV, Liu S, Leppla SH. Identification of a receptor-binding region within domain 4 of the protective antigen component of anthrax toxin. Infect. Immun 1999;67:1860–1865. [PubMed: 10085028]
20. Klimpel KR, Arora N, Leppla SH. Anthrax toxin lethal factor contains a zinc metalloprotease consensus sequence which is required for lethal toxin activity. Mol. Microbiol 1994;13:1093–1100. [PubMed: 7854123]
21. Puente XS, Sanchez LM, Overall CM, Lopez-Otin C. Human and mouse proteases: a comparative genomic approach. Nat. Rev. Genet 2003;4:544–558. [PubMed: 12838346]
22. Dhanasekaran SM, Barrette TR, Ghosh D, Shah R, Varambally S, Kurachi K, Pienta KJ, Rubin MA, Chinnaiyan AM. Delineation of prognostic biomarkers in prostate cancer. Nature 2001;412:822–826. [PubMed: 11518967]
23. Ullmann R, Morbini P, Halbwedl I, Bongiovanni M, Gogg-Kammerer M, Papotti M, Gabor S, Renner H, Popper HH. Protein expression profiles in adenocarcinomas and squamous cell carcinomas of the lung generated using tissue microarrays. J Pathol 2004;203:798–807. [PubMed: 15221939]
24. Wasenius VM, Hemmer S, Kettunen E, Knuutila S, Franssila K, Joensuu H. Hepatocyte growth factor receptor, matrix metalloproteinase-11, tissue inhibitor of metalloproteinase-1, and fibronectin are up-regulated in papillary thyroid carcinoma: a cDNA and tissue microarray study. Clin Cancer Res 2003;9:68–75. [PubMed: 12538453]
25. Hoang CD, D'Cunha J, Kratzke MG, Casmey CE, Frizelle SP, Maddaus MA, Kratzke RA. Gene expression profiling identifies matriptase overexpression in malignant mesothelioma. Chest 2004;125:1843–1852. [PubMed: 15136399]
26. Kang Y, Siegel PM, Shu W, Drobnjak M, Kakonen SM, Cordon-Cardo C, Guise TA, Massague J. A multigenic program mediating breast cancer metastasis to bone. Cancer Cell 2003;3:537–549. [PubMed: 12842083]
27. Coombs GS, Bergstrom RC, Pellequer JL, Baker SI, Navre M, Smith MM, Tainer JA, Madison EL, Corey DR. Substrate specificity of prostate-specific antigen (PSA). Chem. Biol 1998;5:475–488. [PubMed: 9751643]
28. Rosovitz MJ, Schuck P, Varughese M, Chopra AP, Mehra V, Singh Y, McGinnis LM, Leppla SH. Alanine scanning mutations in domain 4 of anthrax toxin protective antigen reveal residues important for binding to the cellular receptor and to a neutralizing monoclonal antibody. J Biol. Chem. 2003

29. Liu S, Leppla SH. Cell surface tumor endothelium marker 8 cytoplasmic tail-independent anthrax toxin binding, proteolytic processing, oligomer formation, and internalization. J. Biol. Chem 2003;278:5227–5234. [PubMed: 12468536]

30. Geran RI, Greenberg NH, MacDonald MM, Schumacher AM, Abbot BJ. Protocols for screening chemical agents and natural products against animal tumors and other biological systems. Cancer Chemother. Rep 1972;3:1.

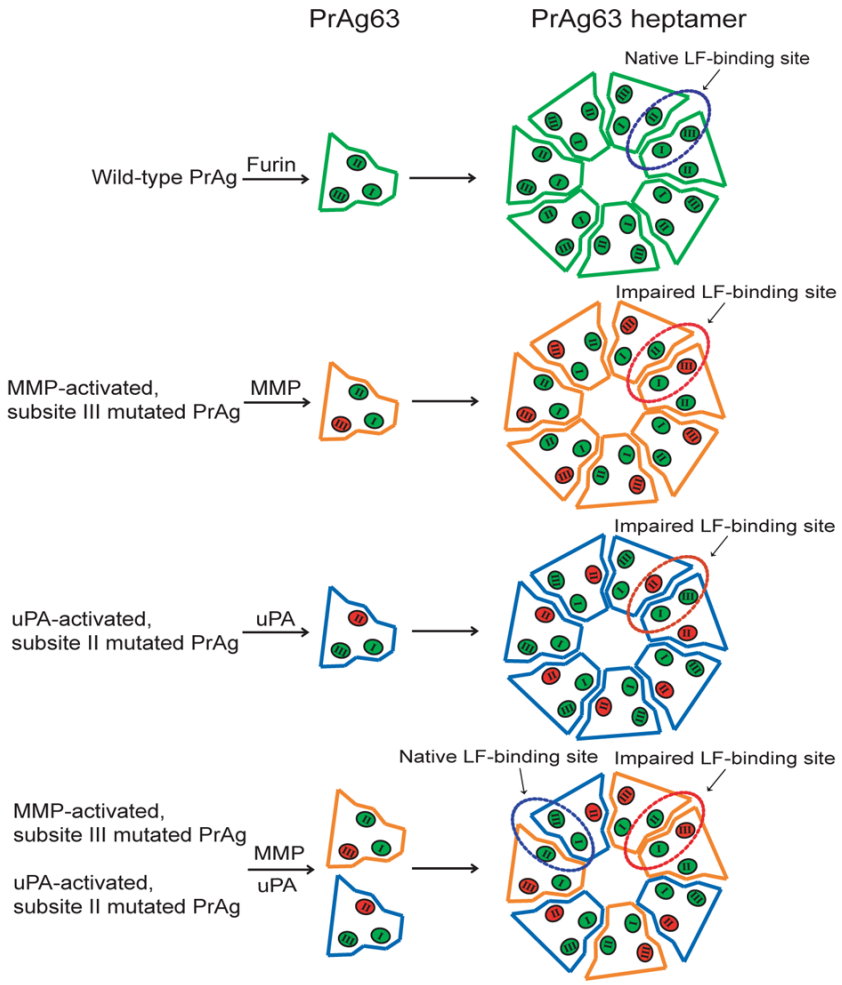

Figure 1.

Schematic representation of intermolecular complementation by mutated PrAg proteins. LF-binding subsites I, II, and III are represented in green as I, II, and III, respectively. LF-binding subsites I and III and subsite II that together comprise one LF-binding site are located on adjacent PrAg63 subunits. Mutations in any of these subsites (shown in red) result in the impaired LF-binding sites on PrAg heptamers. However, up to three active LF-binding sites can be regained by intermolecular complementation of the two PrAg monomers with different LF-binding subsites mutations, such as in II and III as shown in the figure.

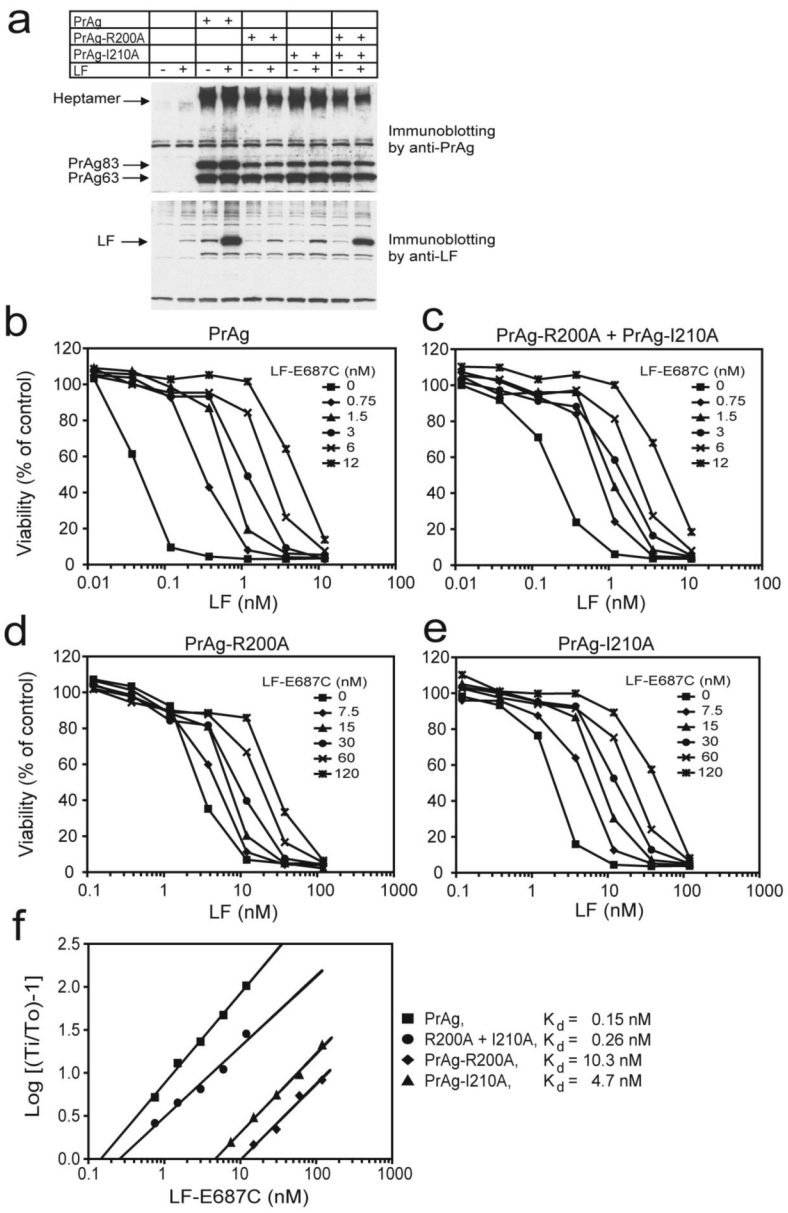

Figure 2.

PrAg proteins with different LF-binding subsite mutations can complement LF-binding and toxicity. **(a)** PrAg-R200A and PrAg-I210A demonstrate intermolecular complementation in mediating LF binding to CHO cells. CHO K1 cells were incubated at 37°C for 2 h with 12 nM of different PrAg proteins (6 nM each of PrAg-R200A and PrAg-I210A when combined) plus 1.2 nM of LF. Cell lysates were analyzed by Western blot for PrAg (top panel) or LF (lower panel). **(b-e)** RAW264.7 cells were incubated at 37°C for 3.5 h with various amounts of LF (0-12 nM) in the presence of 6 nM PrAg **(b)**, 3 nM PrAg-R200A combined with 3 nM PrAg-I210A **(c)**, 6 nM PrAg-R200A **(d)**, and 6 nM PrAg-I210A **(e)**. Different concentrations of LF-E687C as indicated were also added to the cells to perform Schild Plot analyses in **(f)**. Cell viability was determined by addition of MTT as described in Methods. **(f)** Schild Plot analyses. The LF concentrations at midpoints (T_i) on the dose response curves in **(be)** were plotted against LF-E687C concentrations, i.e., Log [(T_i/T_o)-1] versus the nanomolar concentration of LF-E687C (T_o is the value of T_i with no LF-E687C added). The intercepts of the resulting lines

at the points where Log $[(T_i/T_o)-1] = 0$ identify the LF-E687C concentrations equal to the apparent Kds, the affinities of LF-E687C to the heptamers formed by the PrAg proteins.

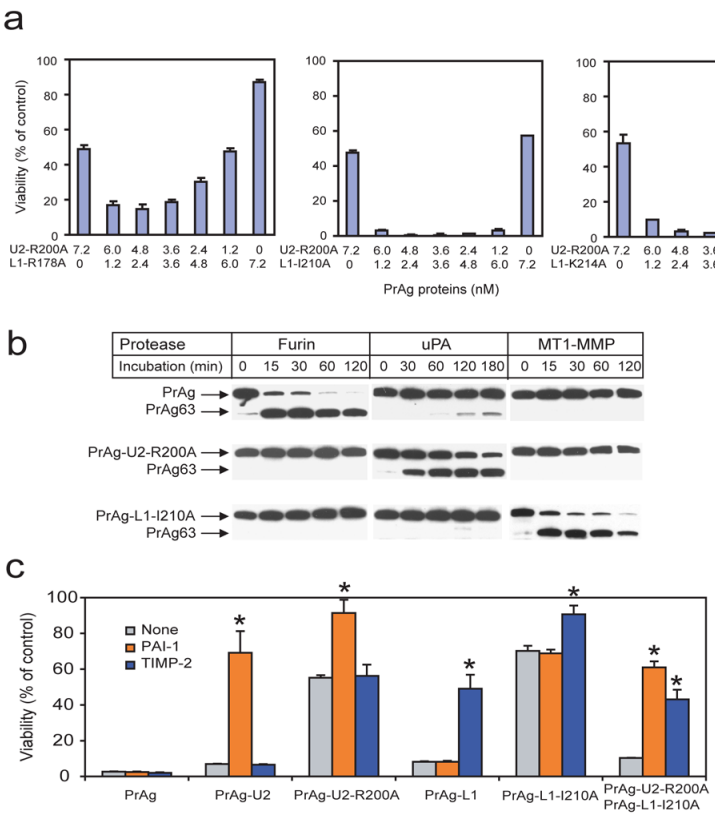

Figure 3.

Efficient killing of human melanoma A2058 cells requires the intermolecular complementation of the two groups of PrAg proteins. **(a)** Human melanoma A2058 cells cultured to 50% confluence were incubated with various ratios of PrAg proteins as indicated together with FP59 (1.9 nM) for 48 h, whereafter MTT was added to determine cell viability. Cytotoxicity to the tumor cells was demonstrated with a wide range of ratios (from 1:5 to 5: 1) of PrAg-U2-R200A and PrAg-L1-R178A, PrAg-U2-R200A and PrAg-L1-I210A, and PrAg-U2-R200A and PrAg-L1-K214A. **(b)** Susceptibility of PrAg, PrAg-U2-R200A, and PrAg-L1-I210A to furin, MT1-MMP, and uPA. PrAg proteins were incubated with the soluble forms of furin and MT1-MMP, and uPA for the times indicated, and then analyzed by SDS-PAGE. The proteins were visualized by Western blotting using an anti-PrAg antiserum (#5308). **(c)** The effects of the protease inhibitors on the cytotoxicity of PrAg proteins to A2058 cells. Human melanoma A2058 cells cultured to 50% confluence were pre-incubated with PAI-1 (46 nM) and TIMP-2 (0.4 μM) for 30 min, then 3.6 nM different PrAg proteins (1.8 nM each for PrAg-U2-R200A and PrAg-L1-I210A when combined) as indicated together with FP59 (1.2 nM) were added for 48 h. MTT was added to determine cell viability at 48 h. *, $p < 0.05$, determined by two-tailed Student's t-test.

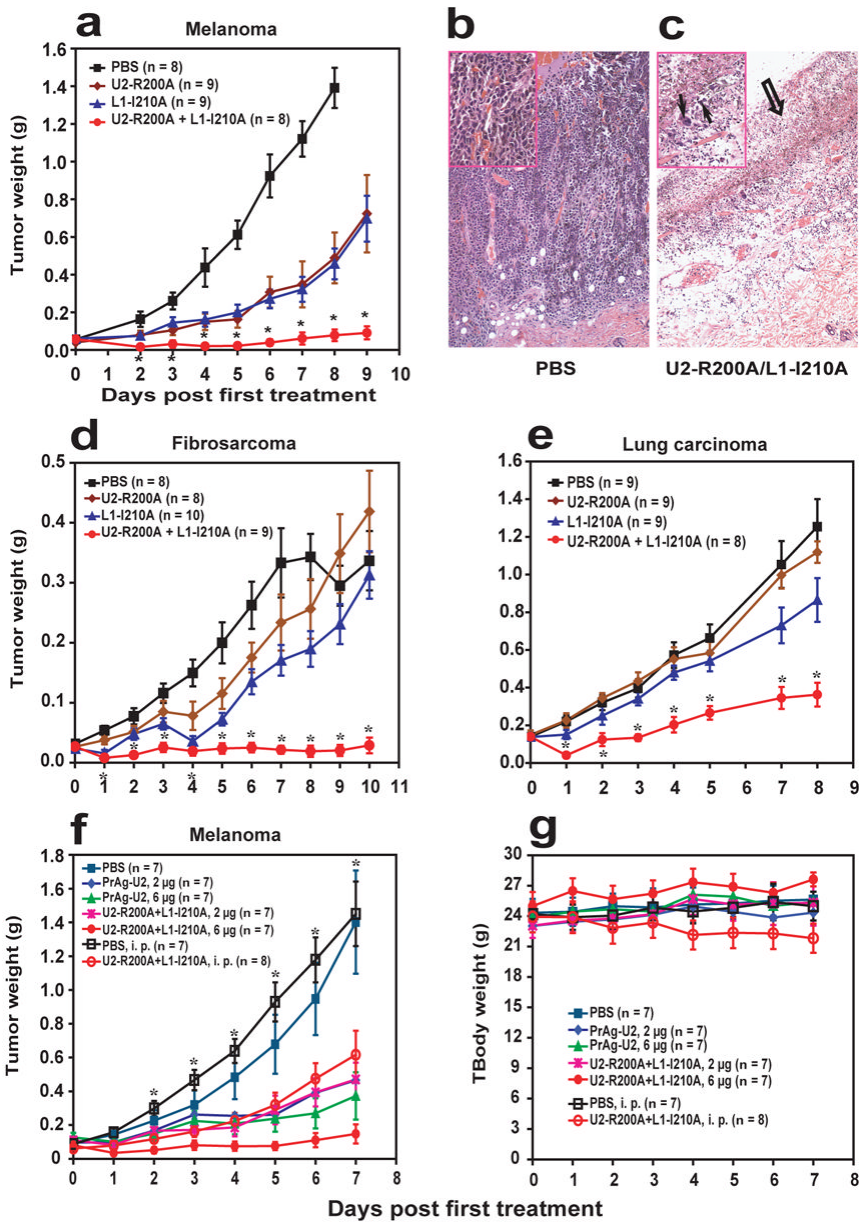

Figure 4.

Potent intermolecular complementation-dependent tumoricidal activity of the engineered PrAg proteins. B16-BL6 melanoma-bearing **(a)**, T241 fibrosarcoma-bearing **(d)**, and LL3 Lewis lung carcinoma-bearing **(e)** mice were injected intradermally adjacent to the tumor nodules with PBS (■), 6 μg PrAg-U2-R200A (▲), 6 μg PrAg-L1-I210A alone (◆), or a combination of 3 μg PrAg-U2-R200A and 3 μg PrAg-L1-I210A (●) in the presence of 0.5 μg FP59 at day 0, 3, and 6. **(b-c)** Microscopic appearance of B16-BL6 melanoma cells 24 h after a single injection of the mice with PBS or the mixture of 3 μg PrAg-U2-R200A, 3 μg PrAg-L1-I210A, and 0.5 μg FP59. Extensive tumor necrosis (empty arrow in **c**, H&E staining, 64×, and insert 160×) and regressive changes, such as karyopyknosis and karyorhexis (arrows in insert) are seen in toxin-treated but not mock-treated tumor **(b**, H&E staining, 64×, insert 160×**)**. **(f)** Comparison of the anti-tumor efficacy of the mutated PrAg proteins. Five groups of B16-BL6 melanoma-bearing mice were treated intradermally with PBS, 2 μg or 6 μg of PrAg-U2 or the

mixture of PrAg-U2-R200A/PrAg-L1-I210A (1 + 1 μg or 3 + 3 μg, respectively) in the presence of 0.5 μg FP59 at day 0, 3, and 6. Two groups of the tumor-bearing mice were treated intraperitoneally with PBS or the mixture of 20 μg PrAg-U2-R200A and 10 μg PrAg-L1-I210A in the presence of 3 μg FP59 at day 0, 3, and 6 (2/3 MTD3). The weight of intradermal tumor nodules is expressed as mean tumor weight ± the SEM. * in **(a)**, **(d)**, and **(e)** represents significance ($p < 0.05$) between the treatments using the combination of PrAg-U2-R200A and PrAg-L1-I210A and using PrAg-U2-R200A or PrAg-L1-I210A alone. * in **(f)** represents significance ($p < 0.01$) between the treatments via i.p. with PBS and the combination of PrAg-U2-R200A and PrAg-L1-I210A.